ESANN 2010 proceedings, European Symposium on Artificial Neural Networks - Computational Intelligence and Machine Learning. Bruges (Belgium), 28-30 April 2010, d-side publi., ISBN 2-930307-10-2.

Neural Oscillations allow for Selective Inhibition - New Perspective on the Role of Cortical Gamma Oscillations

Thomas Burwick

Frankfurt Institute for Advanced Studies (FIAS)
Johann Wolfgang Goethe-Universität
Ruth-Moufang-Str. 1, 60438 Frankfurt am Main, Germany
and
Thinking Networks AG
Markt 45-47, 52062 Aachen, Germany
burwick@fias.uni-frankfurt.de

Abstract. A pattern recognition mechanism is proposed that uses inhibitory oscillations as fundamental ingredient. The mechanism realizes selective inhibition that could not be reached without oscillations. It uses couplings that are motivated by physiology. Since inhibitory oscillations are key to the generation of cortical gamma oscillation, the proposed mechanism may also shed new light on the gamma oscillation functionality.

1 Introduction

Recent years brought increasing evidence that the inhibitory system plays an essential role in the generation of cortical gamma rhythms; see [1] for an article with a recent list of references. Related theoretical considerations mostly dealt with the conditions that cause the inhibitory generation of these rhythms. Here, we take another point of view by studying whether inhibitory oscillations provide a particular benefit with respect to pattern recognition.

In the following, we therefore propose a pattern recognition mechanism that uses inhibitory oscillations as fundamental ingredient. In section 2, we give heuristic arguments for the mechanism. In section 3, we give a concrete model and examples that confirm the pattern recognition capability of the mechanism. To realize the particular effect of the inhibitory oscillation, it turns out to be essential to include a frequency spread of the excitatory units. The chosen couplings are inspired by physiology. Accordingly, the mechanism may also shed new light on the possible functionality of the gamma oscillations.

2 The Shadowing Mechanism: Selective Inhibition

To formulate the mechanism, a few assumptions about the coupling structures have to be made; see [2] for detailed physiological reviews.

Firstly, we consider a network of "columns", where each column consists of an excitatory and an inhibitory unit, each rather representing a set of (biological) neurons. Evidently, we assume mutually excitatory and inhibitory couplings

ESANN 2010 proceedings, European Symposium on Artificial Neural Networks - Computational Intelligence and Machine Learning. Bruges (Belgium), 28-30 April 2010, d-side publi., ISBN 2-930307-10-2.

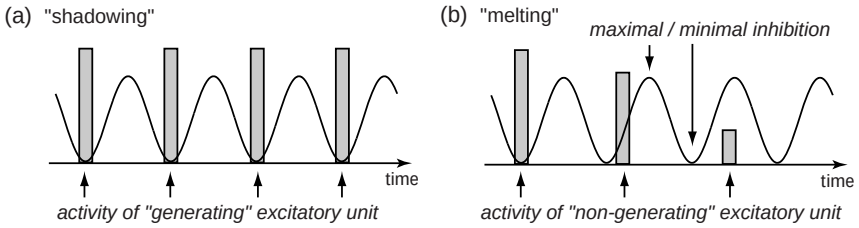

Fig. 1: The oscillatory lines illustrate an oscillation of the inhibitory pool with minimal inhibition whenever the time axis is touched and maxima in between. The rectangles represent tendencies of excitatory units to fire at times, marked through the positions of the rectangles, that are (a) compatible, or (b) not compatible with the inhibitory rhythm, corresponding to the generating and non-generating roles of the units, respectively. In case of (b), the inhibitory effect suppresses the activity, indicated through lower height of the rectangles; see section 2 for more explanations.

between, respectively, excitatory and inhibitory units. Memory of patterns is implemented through these excitatory couplings.

Secondly, each excitatory unit is assumed to excite the inhibitory unit of the same column (this makes the columnar architecture). Thirdly, it is assumed that this specificity is lost in the feedback, that is, the inhibitory units inhibit different (neighboring) excitatory units, so that the excitatory units (in a neighborhood) are subject to inhibition from the same inhibitory pool.

In the following, the frequency of oscillating excitatory activity plays a central role. Without considering the inhibitory effect, the different excitatory units may tend to fire with different frequencies. The most trivial source of such frequency spread (and the one that is illustrated with the example of section 3) is due to different states of activity: on-state units have higher frequencies than off-state units. Moreover, frequency differences between on-state units may be due to Hebbian memory and corresponding pattern frequency-splitting [3].

The frequency spread of possible excitatory oscillations may be crucial when combined with another oscillation that carries its own frequency: the oscillation of the inhibitory pool. This constitutes another drive of the excitatory rhythm since excitatory units tend to be active whenever the inhibitory effect decayed towards a minimum. Then, inhibition is weak and excitatory firing may arise, thereby exciting the inhibitory units of the same column and increasing the inhibitory effect again, and so on, resulting in the oscillatory dynamics; see [4] for a review of the corresponding cortical dynamics, the gamma cycle.

To formulate the combined excitatory and inhibitory dynamics, we need to combine the two oscillatory drives of excitatory dynamics, that is, the one resulting from excitatory dynamics with frequency spread, and the other resulting from the inhibitory pool.

Let us first neglect the frequency spread, that is, we assume that all excitatory

units tend to fire with the same frequency. A balanced situation may then have all excitatory units active with the same frequency at times when the inhibitory effect of the oscillating inhibitory pool is minimal. Figuratively spoken, one may identify the inhibitory effect with some "heat" and, accordingly, one may refer to the timing of the excitatory units as being "in the shadow".

Let us also introduce the notion of "generating" excitatory units: these are the ones that generate the rhythm of the inhibitory pool through exciting the inhibitory unit of there own column. In case of global shadowing, all excitatory units are generating. Their situation may be illustrated as in figure 1a.

Let us now also consider the frequency spread of the excitatory units. In particular, we may assume that only a subset of excitatory units remains generating. The other ones - for example, the ones less strongly driven by excitatory inputs - may just not be able to cope with the frequency of the inhibitory pool. Figuratively spoken, not being able to escape into the shadow, these non-generating excitatory units are "not able to freeze" or "melt away"; figure 1 illustrates this temporally selective inhibition, where the inhibitory effect of the pool on particular excitatory units is stronger (weaker) in panel b (a).

3 Model and Example: Relevance of Frequency Spread

In this section, we sketch an oscillatory neural network model that implements the principles that were described in the foregoing section.

The model may be constructed as complex-valued gradient system, analogously to the construction in [3]. We consider a network with N columns, indexed though $n = 1, ..., N$. In comparison to the model in [3], the essential extension is that each column consists not only of an excitatory units with amplitude $U_n = g(u_n)$, $g(\cdot) = (1 + \tanh(\cdot))/2$, and phase ϕ_n, but also of an inhibitory unit. The latter is described with amplitude $V_n = g(v_n)$ and phase θ_n. Using the approach of [3], the dynamics is given by

$$\widetilde{\tau}_E(u_n)\ \frac{du_n}{dt} = -u_n + I_n - \frac{\partial}{\partial U_n}\left(\mathcal{R}_{EE} + \mathcal{R}_{EI}\right) \tag{1a}$$

$$\frac{d\phi_n}{dt} = \omega_{0,n} + \omega_{1,n}U_n - \frac{2}{\tau_E U_n}\frac{\partial}{\partial \phi_n}\left(\mathcal{R}_{EE} + \mathcal{R}_{EI}\right) \tag{1b}$$

$$\widetilde{\tau}_I(v_n)\ \frac{dv_n}{dt} = -v_n + I'_n - \frac{\partial}{\partial V_n}\left(\mathcal{R}_{IE} + \mathcal{R}_{II}\right) \tag{1c}$$

$$\frac{d\theta_n}{dt} = \omega'_{0,n} + \omega'_{1,n}V_n - \frac{2}{\tau_I V_n}\frac{\partial}{\partial \theta_n}\left(\mathcal{R}_{IE} + \mathcal{R}_{II}\right), \tag{1d}$$

where $\widetilde{\tau}_E(u_n) = (1 - U_n)\ \tau_E$, $\widetilde{\tau}_I(v_n) = (1 - V_n)\ \tau_I$, and τ_E, τ_I are time scales. External inputs are given by I_n, I'_n, the intrinsic frequencies are $\omega_{0,n}$, $\omega'_{0,n}$, while $\omega_{1,n}$, $\omega'_{1,n}$ describe shear parameters.

The gradients in equation 1 describe the couplings. Notice, for sake of simplicity we assumed real-valued gradient functions. These couplings between

excitatory (E) and inhibitory (I) units are then chosen to be in accordance with the assumptions made in section 2:

$$\mathcal{R}_{EE} = -\frac{1}{2N}\sum_{m,n=1}^{N} h_{mn}U_mU_n\left(\alpha+\frac{\beta}{2}\cos(\phi_m-\phi_n)\right) \tag{2a}$$

$$\mathcal{R}_{IE} = -\frac{\gamma}{2}\sum_{n=1}^{N} U_nV_n\cos(\phi_n-\theta_n) \tag{2b}$$

$$\mathcal{R}_{EI} = \frac{\eta}{2N}\sum_{n,m=1}^{N} U_nV_m\left(1-\cos(\phi_n-\theta_m)\right) \tag{2c}$$

$$\mathcal{R}_{II} = \frac{\eta'}{4N}\sum_{n,m=1}^{N} V_nV_m\left(1-\cos(\theta_m-\theta_n)\right) \tag{2d}$$

The coupling constants $\alpha, \beta, \gamma, \eta, \eta'$ are assumed to be real-valued and positive.

The following examples are based on the storage of the $P = 6$ images shown in figure 2a. Each image is represented in terms of Gabor wavelet responses at $L\times L$ lattice points, $L = 32$. At each node of the lattice, the local part of the image is encoded in $N_s \times N_o$ Gabor wavelets responses, where $N_s = 3$ is the number of scales and $N_o = 6$ the number of orientations. We are then dealing with a network of $N = L \times L \times N_s \times N_o$ units. A threshold is used for the magnitude of these responses: each images, indexed through $p = 1, ..., P$, is then represented in terms of components $\xi_n^p \in \{0, 1\}$, with $n = 1, ..., N$. The $4(L-1) \times N_s \times N_o$ values at the image boundary are set to zero to avoid boundary effects. As an illustration of the resulting Gabor representation, we consider a "texture map" that is obtained by summing the components at each node of the lattice; see figure 2b. The image representations, i.e., patterns ξ_n^p are stored according to Hebbian memory as described in [3] with pattern weights $\lambda_p = (\sum_n \xi_n^p)^{-1}$.

Two examples are considered, characterized through

$$\text{example 1: } \beta = 0,\ \omega_{1,n} = 0 \quad , \quad \text{example 2: } \beta = 0,\ \omega_{1,n} > 0, \tag{3}$$

with $\omega'_{1,n} = \omega_{1,n}$. The choice $\beta = 0$ implies that there is no direct synchronizing interaction between excitatory units. Thus, any synchronization observed in the following is due to inhibitory effects! Example 1 is then used to confirm that such synchronization is indeed possible, based on the dynamics given by equations 1 and 2.

The remaining parameters are chosen to be $\tau_E = \tau_I = \tau = 1, \omega_{0,n} = \omega'_{0,n} = 0$, $\alpha = 10$, $\gamma = \eta = \eta' = 8\pi$. As input image, we choose the one displayed in figure 2c, respresented in terms of corresponding thresholded Gabor responses, $\xi_n^{\hat{\text{input}}} \in \{0, 1\}$. This image in then encoded into inputs I_n, I'_n that suppress activity in the network at units n, where $\xi_n^{\hat{\text{input}}} = 0$. Notice,

$$\lambda_4\sum_{n=1}^{N}\xi_n^{\hat{\text{input}}}\xi_n^4 \simeq 69\% \ > \ \lambda_3\sum_{n=1}^{N}\xi_n^{\hat{\text{input}}}\xi_n^3 \simeq 36\% \ > \ \lambda_q\sum_{n=1}^{N}\xi_n^{\hat{\text{input}}}\xi_n^q \tag{4}$$

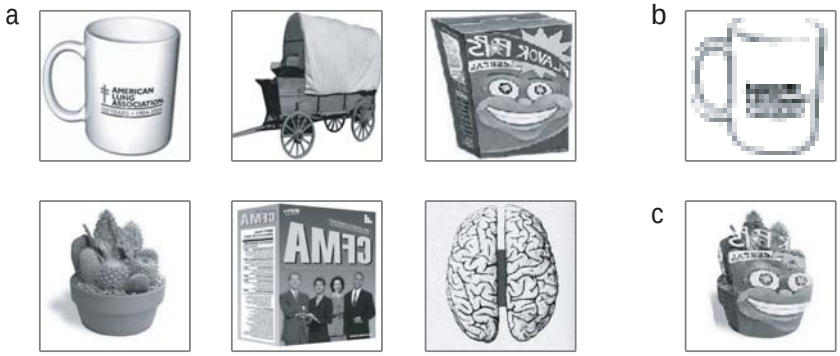

Fig. 2: (a) The set of $P = 6$ stored images, showing a cup ($p = 1$), wagon ($p = 2$), cereal box ($p = 3$), cactus ($p = 4$), another cereal box ($p = 5$) and a brain ($p = 6$). The images are taken from the Caltech-256 image collection [5]. (b) Texture map of image $p = 1$ at resolution $L \times L$, where $L = 32$. White pixels illustrate lattice nodes where none of the thresholded Gabor responses is non-vanishing, black pixels show nodes where $N = N_s N_o = 18$ are non-vanishing, values in between are gray (here, the maximum is 17). (c) Input image used for the examples, constructed from $p = 3$ and $p = 4$.

for $q = 1, 2, 5, 6$ $(15\%, 17\%, 14\%, 16\%)$. Accordingly, a reasonable competition among the stored images should lead to image $p = 4$ (the cactus) as winner.

To study the collective dynamics, we consider the activity A_{cactus} and coherence C_{cactus} (degree of synchronization) of the set of excitatory units given by $\xi_n^{\text{input}} = \xi_1^4 = 1$. The activity and coherence of units with $\xi_n^{\text{input}} = 1$ but $\xi_1^4 = 0$ are referred to as A^c_{cactus} and C^c_{cactus}. To display the results of example 1, we also use global coherence C, describing the synchronization of all units with $\xi_n^{\text{input}} = 1$. Exact definitions of these quantities are obtained in analogy to the definitions given in [3].

The results of example 1 are displayed in figure 3a-c. Initially, the inhibition is diffuse (coherence of excitatory and inhibitory units are nearly identical, due to equation 2b). The cactus component gets active, the corresponding units are therefore becoming the generating ones, while the complement is inhibited at the beginning. Then, however, the complement takes the rhythm of the coherent inhibitory pool, it moves "into the shadow" of inhibition and "recovers" from the initial suppression, so that finally a state of "global shadowing" is reached. This is indicated through the broken line in figure 3a and the global coherence as displayed in figure 3b. The result confirms that synchronization may be implied through the described set of inhibitory couplings, without using synchronizing couplings between excitatory units.

Example 2 uses the same initial values and parameters as the first example, except for including a frequency spread resulting from shear. Due to this frequency spread, the deactivated units are no longer able to cope with inhibi-

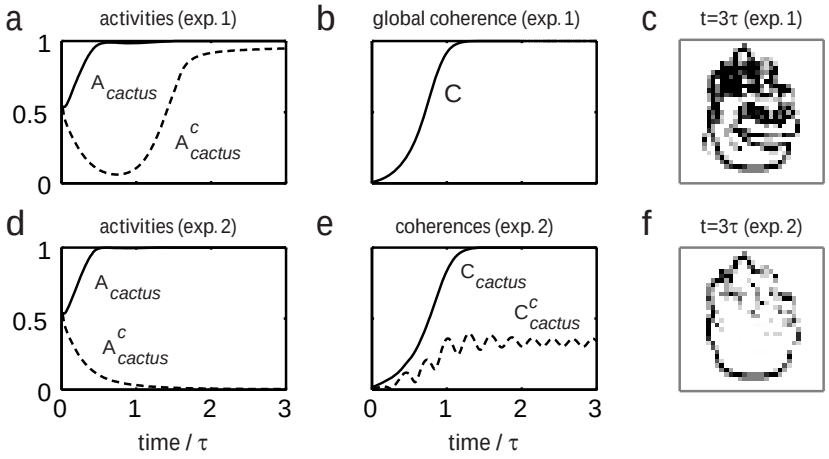

Fig. 3: (a-c) Example 1, (d-f) example 2; see section 3. Comparing the texture maps of activities V_n at $t = 3\tau$ in (c) and (f) confirms the recovery of the cactus pattern in example 2 (black pixels now correspond to values $\geq N_s N_o/2$, white pixels indicate vanishing value and gray pixels indicate values in between).

tion through taking the rhythm of the inhibitory pool; see figure 3d-f. While the generating units, i.e., the ones that fuel the inhibitory pool, may live in its "shadow", see figure 1a and the solid line in figure 3d, the other units are driven by other frequencies, bringing these into conflict with inhibition ("heat"). This conflict prevents these units from "freezing" into an active and coherent state (corresponding to "melting" if the initial configuration is already in such a state), see figure 1b and the broken line in figure 3d.

In summary, it can be stated that the model of equations 1 and 2 shows a form of temporally selective inhibition, confirming the arguments of section 2.

References

[1] Christoph Börgers and Nancy J. Kopell. Gamma oscillations and stimulus selection. *Neural Computation*, 20:383–414, 2008.

[2] Gordon M. Shepherd. *The Synaptic Organization of the Brain.* Oxford University Press, New York, fifth edition, 2004.

[3] Thomas Burwick. Temporal coding: Assembly formation through constructive interference. *Neural Computation*, 20:1796–1820, 2008.

[4] Pascal Fries, Danko Nicolić, and Wolf Singer. The gamma cycle. *Trends in Neurosciences*, 30(7):309–316, 2007.

[5] G. Griffin, A. Holub, and P. Perona. Caltech-256 object category dataset. Technical Report 7694, California Institute of Technology, 2007.